J. Jpn. Soc. Microgravity Appl. Vol. 28 No. 2 2011 (S120–S125)

8th Japan-China-Korea Workshop on Microgravity Sciences for
Asian Microgravity Pre-Symposium

Investigation of Gas-Liquid Interface Behavior on Propellant Reorientation in Microgravity Environment

Zhangguo LI, Qiusheng LIU* and Rong LIU

Abstract

The computational and experimental studies have been performed to investigate the process of liquid propellant reorientation flow dynamics for the tank of CZ-3A launch vehicle series fuel tanks in microgravity environment. The volume-of-fluid (VOF) method was used to simulate the free surface flow of gas-liquid. The process of the liquid propellant reorientation started from initially curved interfaces. The characteristic time of propellant reorientation flow was obtained from numerical simulation. The results agree well with the experiments. It's found that the method of small thrust for liquid reorientation is effective and thrust impulse consumption for reorientation could be saved by using a small thrust Bond number. In addition, a series experimental investigation was conducted in the Drop Tower Facility of National Microgravity Laboratory of China. Preliminary drop tower experimental results shows that the sponge PMD is effective in holding the liquid in microgravity environment..

1. Introduction

In order to fit different transmission requirements, the main engine of launch vehicle must have the ability to restart more than two times in microgravity environment. During the engine-off time, the liquid propellant is expected to be held in the proper position of the tank for an engine restart on the vehicle. On earth, liquid in a tank settles to the bottom to minimize is gravitational potential energy. In space, where the effective gravity is small, the location of liquid in a tank is determined by the competing effects of gravity and the liquid's surface tension, and the shape of the free surface in the tanks is also strongly impacted by one parameter, the angle between the gas-liquid phase boundary and the solid container wall at the contact line [1),2)], except in the situation of the gravity or tank scale large enough. In order to minimize the sum of the gravitational and surface energies.[3)] Spacecraft must therefore complement methods to ensure that the liquid is located at the desired location in the tank even when effective gravity is directed adversely or in unknown directions. Similarly, if the tank is pressurized and must be vented periodically, methods are required to ensure that gas is positioned over the vent. In recent years, NASA has planned the on-orbit management [4)] of liquid hydrogen for the return to the moon [5)]: the extended storage and handling of large quantities of liquid hydrogen on-orbit. CZ-3A launch vehicle series [6)] is the rocket series with the largest carrying capacity in China at present and the main large commercial rocket series. It is mainly used to launch the geostationary transfer orbit (GTO) payload, low earth orbit (LEO) payload and sun synchronous orbit (SSO) payload as well as payloads flying to the moon and Mars can also be launched. The worst case of propellant reorientation is that the liquid phase locates at the top of the tank. Various methods have been proposed to control the location of the liquid for engine venting and restarting. In the present design of large propellant tanks, one way to accomplish both of these objectives is to use an auxiliary thrusting system to provide a linear acceleration large enough to settle the liquid. Its principles are similar to a tank on Earth exposed to gravity. With the CZ-3A launch vehicle series, a typical upper-stage vehicle, four 10-N and four 150-N thrusters are used to settle the propellant in the tank. So, the thrust and time required to reorient the liquid propellant back to its desired location must be known to ensure a successful engine restart sequence and to determine effective thruster parameters. Another method is to in corporate passive systems or devices that increase the effective surface tension forces sufficiently to hold the liquid at the desired position against adverse accelerations. These systems have been given the general name of propellant management devices (PMDs) [7)].

2. Numerical Model Description

In recent years, a number of methods have been developed for modeling such free surface flows [8)], which can be classified primarily as Lagrangian or Eulerian-based. Eulerian-based methods are better suited for flows with complex topological changes and interface deformations. The volume-of-fluid (VOF) method [9)] is an Eulerian based method that has been widely used. It utilizes a volume fraction function to track the interface implicitly. In this method, a scalar function F is defined as the

Key Laboratory of Microgravity (National Microgravity Laboratory), Institute of Mechanics, Chinese Academy of Sciences, Beijing 100190, China
(E-mail: liu@imech.ac.cn)

fraction of a cell volume occupied by fluid. F is assumed to be unity when a cell is fully occupied by the fluid and zero for an empty cell. Cells with values of 0 < F < 1 contain a free surface.

In this paper, an axisymmetric model is adopted for the unsteady, incompressible flows with deforming free surfaces in which surface tension forces are significant in microgravity. For incompressible flows with constant properties, the continuity, momentum and VOF equations are given by:

$$\nabla \cdot \mathbf{v} = 0 \tag{1}$$

$$\frac{\partial}{\partial t}(\rho \mathbf{v}) + \rho(\mathbf{v}\cdot\nabla)\mathbf{v} = -\nabla p + \mu \nabla^2 \mathbf{v} + \vec{\mathbf{F}}_s + \rho \vec{\mathbf{a}} \tag{2}$$

$$\frac{\partial F}{\partial t} + \mathbf{v}\cdot\nabla F = 0 \tag{3}$$

The symbol $\mathbf{v}$ is the velocity vector; p, ρ, and μ represent the pressure, density, and viscosity of the mixture fluid, respectively. F is the VOF function. The term **a** denotes the residual acceleration of the aerodynamic drag acting on the spacecraft for the orbital maneuver course; $\mathbf{F}_s$ is the surface tension at the liquid–gas interface Surface tension effect plays a significant role in the free surface flow problems in micro-gravity environment. The continuum surface force (CSF) model [10] has been widely used to model surface tension. In the CSF model, surface tension effect is treated as a body force $\mathbf{F}_s$, It is distributed within a transition region of finite thickness at the interface, given by:

$$\vec{\mathbf{F}}_s = \sigma \kappa \vec{\mathbf{n}} \delta(\vec{\mathbf{x}}) \tag{4}$$

where σ is the coefficient of surface tension, κ the mean curvature, **n** the normal to the surface, and $\delta(\mathbf{x})$ a delta function concentrated at the interface. In the context of the VOF method, the body force is given by:

$$\vec{\mathbf{F}}_s = \sigma \kappa \nabla F \tag{5}$$

It is included in the momentum equation as a source term. This continuum treatment of the discontinuous change at the interface eases the implementation of the surface tension effect where only the VOF function is needed. In problems with complex topological changes, the CSF model is superior to the conventional method in robustness and versatility. The term $\sigma\kappa\nabla F$ indicates that $\mathbf{F}_s$ is proportional to the curvature κ with the force acting along the normal direction of the interface. Contact angles are applied as a boundary condition at the contact line [11]. In the simulation, we set the contact angle $\theta_c = 0$. Boundary conditions for fluid along solid surfaces are the no-slip and no-penetration conditions.

For the following simulations, the body force weighted scheme is utilized to compute the face pressure by assuming that the normal gradient of the difference between pressure and body forces is constant. The pressure-implicit with splitting of operators (PISO) [12], pressure– velocity coupling scheme is used to obtain a semi-implicit pressure correction equation. The pressure-correction equation is subsequently solved using the algebraic multigrid (AMG) method [13]. Temporal discretization is accomplished using implicit time integration, which is unconditionally stable with respect to time step size. Solutions are subsequently iterated at each time level until the convergence criteria are met. The geometric reconstruction scheme is used to reconstruct the interface between fluids using a piecewise-linear approach.

3. Model Verification and Validation

The cases of Lewis Research Center drop tower model [14] was chosen to verify and validate the program. The experiment test containers were right-cylinders machines from II UVA acrylic plastic with spheroidal tops and inverted spheroidal bottoms to scale a Centaur-space-vehicle, liquid hydrogen tank. The model tanks used had radii R of 5.5 and 7.0 centimeters and length L_1 of 21.8 and 27.8 centimeters, respectively. FC-78 was used as test liquid. Surface tension, density, and viscosity of FC-78 are presented in **Table 1**.

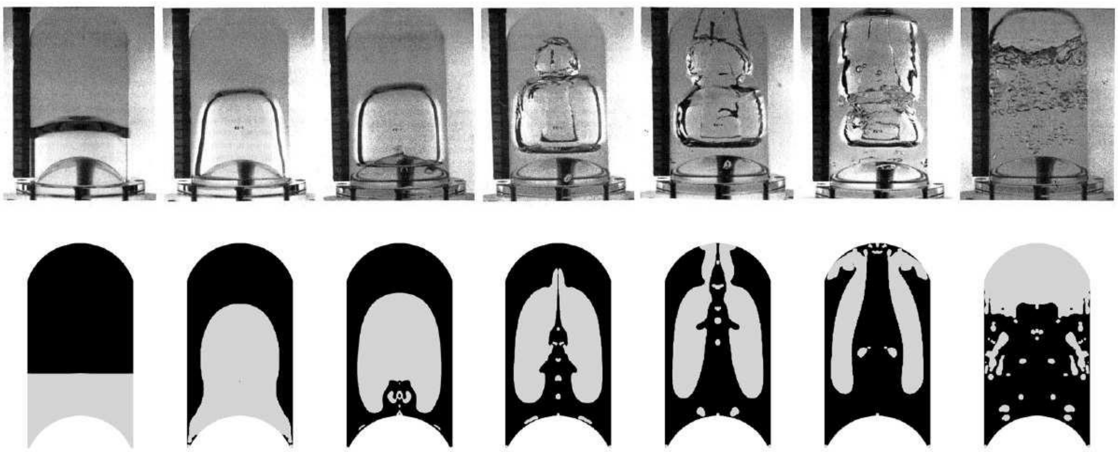

Fig. 1 Reorientation flow process of scale model Centaur experiment compared with simulation for drop tower

Table 1 Properties of FC-78 at 20℃ [14]

Liquid	σ, N/m	ρ, kg/m^3	μ, kg/m·s
FC-78	13.2×10^{-3}	1720.0	8.2×10^{-3}

Table 2 Reorientation event data

Liquid fill, percent			20	20	70
Reorientation acceleration, **a**, cm/sec^2			31	69	31
Reorientation event times, sec	T_1	Calculated	1.23	0.84	0.77
		Measured	1.23	0.85	0.78
	T_2	Calculated	1.30	0.93	1.01
		Measured	1.34	0.94	0.96
	T_3	Calculated	------	------	1.39
		Measured	------	------	1.23
	T_4	Calculated	1.70	1.16	1.48
		Measured	1.72	1.29	1.55
	T_5	Calculated	5.45	3.10	3.59
		Measured	>2.54	2.50	>2.51

In **Fig.1**, the black region indicates liquid phase area, and the gray region indicates gas phase area. And as **Fig.1** shown above, a series event times from initiation of thrust [14] were defined as below for the reorientation process.

T_1: time of liquid impact at tank bottom

T_2: time of geyser initiation

T_3: time of geyser impact on liquid-vapor interface

T_4: time of geyser impact on tank top

T_5: time when tank top is clear of liquid

Three cases of the reorientation model experiment were investigated and the event times were obtained by simulation. As shown in **Table 2**, the calculated results are in good agreement with the experiment measured results.

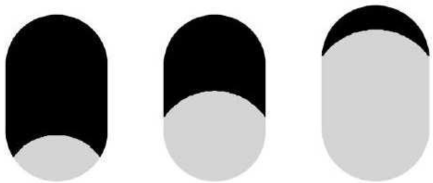

Fig. 2 Initial gas-liquid interface profiles prior to reorientation at liquid fill ratio 80%, 50%, 10%

4. Numerical Results and Discussions

Theoretical analyses of liquid behavior in microgravity [15),16)] indicate that the initial state of the gas-liquid interface should be a curved surface under micro-gravity condition. The general solution for the equilibrium gas-liquid interface shape is described by the Bond number ($Bo = \rho \mathbf{a} R^2/\mu$, **a** is the residual acceleration; R is the radius of the tank), an indicator of the size of the inertia forces to interfacial forces. During the reorientation process, the initial conditions of the gas-liquid interface will determine the flow mode of liquid in fuel tanks [17)]. According to the on-orbit vehicle situation, the liquid was stabilized at the top of the tank at a Bond number of 10 with a curved interface as shown in **Fig.2**. Here the black area denotes liquid, the gray denotes gas. The engine would restart in a number of times with different propellant residual, and three different propellant fill ratios were selected to simulate each stages of reorientation.

The tank here has a concave spherical bottom inside that is different form the convex spheroidal bottom of Centaur scale model. As the characteristic times defined previously, the time T_1 equals to T_2 in these cases. In additional, we define T_6 as the time that all the bubbles discharged from the liquid which almost reached equilibrium state. In the condition of reorientation Bond number of 393.0, the specific reorientation flow process is shown in **Fig.3**. Initially, the propellant gas-liquid interface had a concave curvature. During the reorientation progress, the liquid propellant shifted down along the tank wall by the application of thrust. Then the geysering occurred when it impacted the tank bottom. The geyser kept moving due to inertia and geyser tip impacted on the interface then reached the top. In these periods, the single gas-liquid interface broke up, gas liquid mixed and bubbles generated from

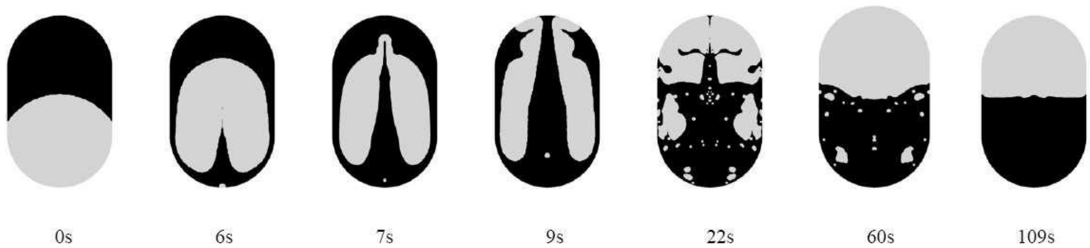

Fig. 3 Reorientation process with initial curved interface (Bo=393.0)

the liquid inside. After the liquid sloshing and bubbles rising, tank top could be clear of liquid. Finally, all the bubbles discharged from the liquid by the settling thrust, the propellant reorientation flow process finished. In the other settling thrusts which were available by the vehicle engine and with liquid fill ratio of 80% and 10%, the flow processes were similar. The difference was that, with higher fluid fill ratio (80%), there were more bubbles generated and gas-liquid mixing more strongly.

Figures 4, 5 and **6** present the propellant reorientation event-time corresponding to the settling Bond number. The results indicate that, The event-time T_1 become the same decrease trend when the settling Bond number increase in different liquid fill ratio cases. Since T_1 is the time of the liquid shifts along the tank wall and impact at the bottom, during this period, the liquid is in a smooth flow state. So T_1 has a simply relationship with the acceleration characteristic and the distance between the liquid interface and the tank bottom. Variation of the time T_5 is similar to T_1. In each case, with the increases of the settling Bond number, T_5 decreases. Because T_5 represents the time of liquid migrate from the tank top to the bottom. Larger settling thrust leads to larger liquid shifting velocity, and the entire migration process of the liquid propellant can be shorter. But under the different fluid fill ratio, the time T_6 shows a different variation to the former. At different fluid fill rate, it shows completely opposite trend. With the liquid flow level 10%, the time T_6 decreases when the settling Bond number increases. But with the liquid flow level 80%, the time T_6 does increase. Since from T_5 to T_6, the process of this period performs the bubbles rise and discharge from the liquid includes the liquid sloshing and bubbles break up and coalescence. With higher fluid fill ratio (80%), there are a large amount of bubbles generated from the liquid when settling thrust get large. It means gas and liquid can mix more strongly in the tank in larger settling Bond number. The flow is considerably chaotic in such a flow motion. So it takes a longer time to be quiescence when the Bond number increases. Conversely, with lower fluid fill ratio (10%), since there are not many bubbles generate in the flow process, and the liquid can quickly reach the equilibrium state without taking long time to discharge bubbles inside.

In the engineering application of on-orbit vehicle tank propellant reorientation, the reorientation time is not the only considered factor. The more important parameter is the impulse consumption of reorientation. Consider the time T_6 defined as mention above to be the time when all the liquid is collected or completely reoriented. We can get the reorientation impulse at different settling Bond number with different liquid fill ratio.

Figure 7 shows that the reorientation impulse and settling Bond number in each case have approximatively a linear relation. The settling Bond number gets larger; the greater impulse for reorientation is needed to settle the liquid propellant.

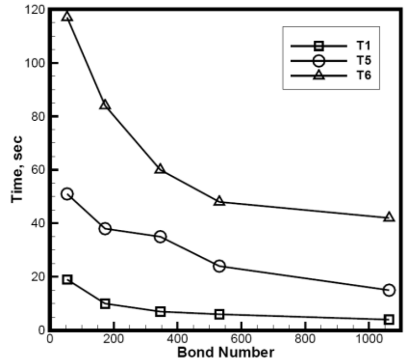

Fig. 4 Reorientation event-time at different settling Bond number, liquid fill ratio 10%

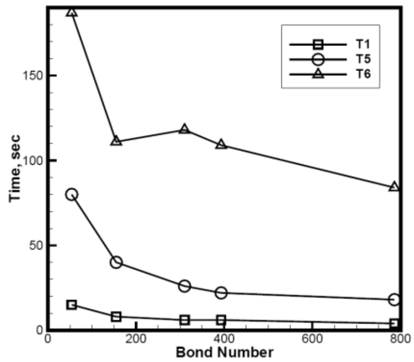

Fig. 5 Reorientation event-time at different settling Bond number, liquid fill ratio 50%

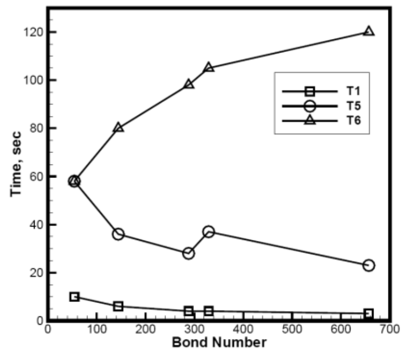

Fig. 6 Reorientation event-time at different settling Bond number, liquid fill ratio 80%

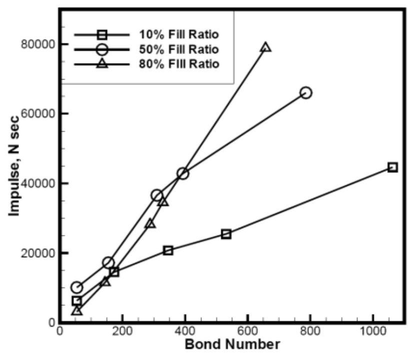

Fig. 7 Reorientation impulse at different settling Bond number with different liquid fill ratio

5. Experimental Setup

The experimental investigation was conducted in the Drop Tower Facility of National Microgravity Laboratory of China (NMLC) with a scale model of liquid propellant tank. Data were obtained by allowing a group of drop cabin (external cabin and internal cabin) (**Fig.8**) to free fall from ground level down a chamber approximately 83 meters deep. This resulted in about 3.6 seconds of free-fall time. By evacuating the external cabin to a pressure below 30 newtons per square meter (3.0×10^{-4} atm), the equivalent gravitational acceleration acting on the experiment platform in the internal cabin due to residual air drag was less than 10^{-5}g. The first step of the experiment purpose was to observe the flow motion of the liquid in microgravity environment without and with PMD sponge. Then next step, reorientation.

The sponge type PMD [18] is a device provides gas free propellant delivery by controlling propellant within the tank. The experimental model tanks of the system are made of plexiglass. The model tanks have the diameter of 110mm. And graphics were collected from the experiments by CCD cameras system which was contained on the experiment platform (**Fig.9**).

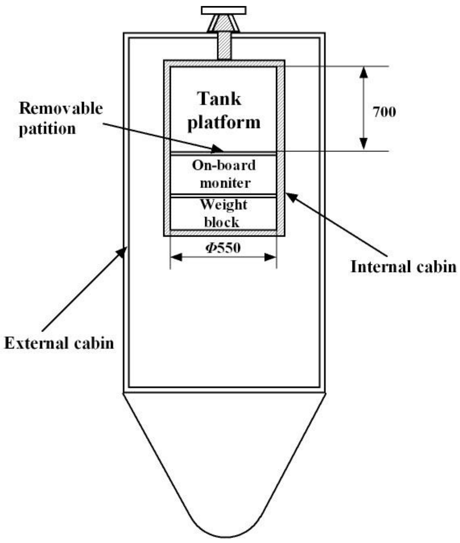

Fig. 8 Experiment cabin for microgravity tests

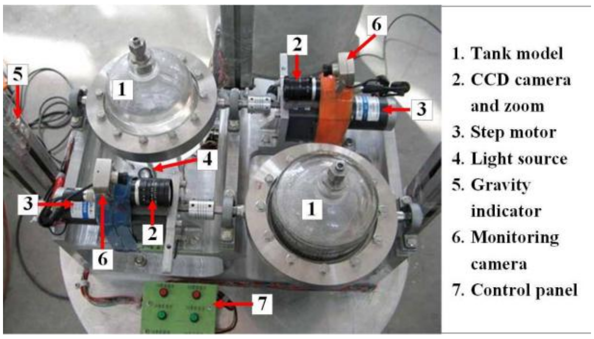

Fig. 9 Model tank platform of drop tower experiment

6. Experimental Results and Discussions

Liquid ammonia and alcohol were used as experimental mediums and the tank free-fall in the drop tower facility. A series of photographs were taken from the drop tower experiment cases. The drop tower experiment data presented is very simply and straightforward. **Figs. 10, 11** illustrate the general behavior of the liquid media in microgravity environment. The liquid quickly climb along the tank and in a spherical formation with the gas in the center. Volume force can't be enough for bounding the liquid in the microgravity environment. In order to hold the liquid phase in the tank bottom, and in the next experiments, we installed the sponge PMD (**Figs. 12, 13**). in the tank bottom to verify the differences with the previous experimental results. The height of sponge PMD is 2/3 of the tank height. With the sponge PMD in the tank, it can be clearly seen that liquid is held in the tank bottom during the tank in the free-fall period instead of flowing along the tank wall to surround the gas (**Figs. 12, 13**). The liquid is held firmly in the entire process in the microgravity condition. These results indicate the sponge PMD is robust in propellant management especially in hold the liquid in microgravity environment. These cases were to understand the performance of liquid behavior in the tank with and without PMD. The remaining experiments of liquid reorientation and the experiment event-time verification are carrying out over the next work.

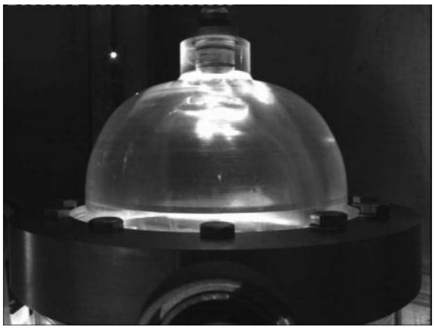

Fig. 10 Liquid ammonia profile in the free-fall state(t= 3.5s)

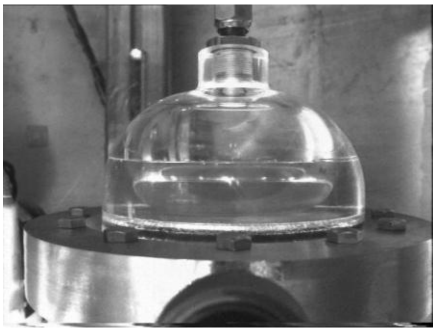

Fig. 11 Alcohol profile in the free-fall state (t = 3.5s)

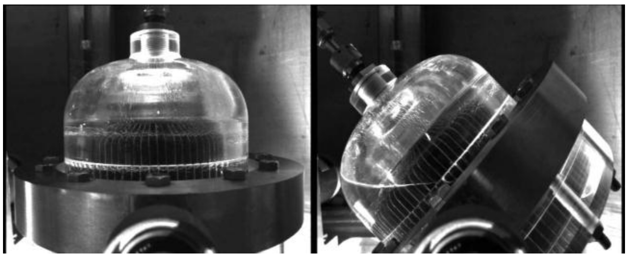

Fig.12 Alcohol profile prior to the free-fall, tank with sponge PMD (t = 0s)

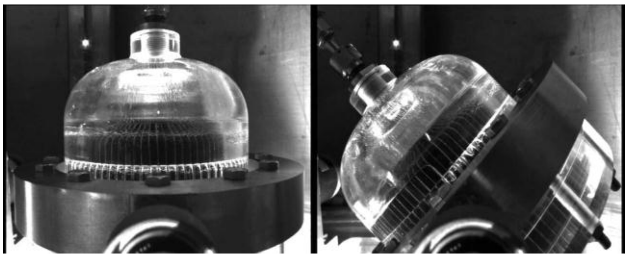

Fig. 13 Alcohol profile prior in the free-fall state, tank with sponge PMD (t = 3.5s)

7. Conclusion

The process of liquid propellant reorientation flow dynamics in microgravity environment is investigated. The VOF method was used to simulate the free surface flow of gas-liquid. The reorientation event-time of propellant reorientation flow was obtained from numerical simulation. The results show that the completely reorientation time behaves different trend at different fluid fill rate. The time T_6 decreases with low fluid fill ratio and increases with high fluid level when the settling Bond number increases. And the greater impulse for reorientation is needed to settle the liquid propellant when the settling Bond number gets larger. Thrust impulse consumption for reorientation could be saved by using a small thrust Bond number. In microgravity environment, the sponge PMD can increase the effective surface tension forces sufficiently to hold the liquid. Take this system into the propellant tank will be useful and effective for propellant management.

Acknowledgement

This research was financially supported by the National Natural Science Foundation of China (Grant Nos. 11072249) and the Knowledge Innovation Project of Chinese Academy of Sciences (CXJJ-10-M55).

References

1) Krahl, R., Gerstmann, J., Behruzi, P., Bansch, E. & Dreyer, M. E., Dependency of the apparant contact angle on nonisohermal conditions, Phys. Fluids, **20** (2008) 042101.
2) Luppes, Helder & Veldman, The numerical simulation of liquid sloshing in microgravity, European Conf. Compulational Fluid Dynamics ((Eds.) Wesseling et al.), 2006.
3) Dodge, F. T.: Low-Gravity Fluid Dynamics and Transport Phenomena. Aeronautics and Astronautics, **130** (1990) 3.
4) Moran, M. E.: Liquid Hydrogen Sensor Considerations for Space Exploration. NASA/TM 2006-214264, 2006
5) NASA: NASA's Exploration Systems Architecture Study. NASA/TM 2005-214062, 2005
6) Long, L. H.: CZ-3A Launch Vehicle Series. Missiles and space vehicles, **239** (1999) 1
7) Ducret, E., Le Moullec, L., Spencer, B., Balaam, P.: Propellant management device studies, computational methods and neutral buoyancy tests. AIAA 92-3611, 1992
8) Scardovelli, R., Zaleski, S.: Direct numerical simulation of free-surface and interfacial flows. Annu. Rev. Fluid. Mech., **31** (1999) 567C603.
9) Hirt, C. W., Nichols, B. D.: Volume of fluid (VOF) method for the dynanlics of free boundaries. J. Comput. Phys. 39, 201-225(1981)
10) Brackbill, J. U., Kothe, D. B., Zemach, C.: A continuum method for modeling surface tension. J. Comput. Phys., **100**(2) (1992) 335C354.
11) Bussmann, M., Mostaghimi, J., Chandra, S.: On a three dimensional volume tracking model of droplet impact [J]. Phys. Fluids, **11**(6) (1999) 1406.
12) Issa, R. I.: Solution of Implicitly Discretized Fluid Flow Equations by Operator Splitting. J. Comput. Phys., **62** (1986) 40.
13) Hutchinson, B. R., Raithby, G. D.: A Multigrid Method Based on the Additive Correction Strategy. Numerical Heat Transfer, **9** (1986) 511.
14) Salzman, J. A., Masica, W. J., Lacovic, R. F.: Low-gravity reorientation in a scale-model Centaur liquid-hydrogen tank. NASA TN D-7168, 1973.
15) Stark, J. A., Bradshow, R. D., Blatt, M. H.: Low-g fluid behavior technology summaries. NASA-CR-134746, 1974.
16) Dodge, F. T.: Further studies of propellant sloshing under low gravity conditions. NASA-CR-119892, 1971.
17) Li, Z. G., Liu, Q. S., Liu, R., Hu,W., Deng, X. Y.: Influence of Rayleigh-Taylor Instability on Liquid Propellant Reorientation in a Low-Gravity Environment. Chinese Phys. Lett., **26** (2009) 114701.
18) Jaekle, D. E., Jr.: Propellant management device conceptual design and analysis: sponges. AIAA 93-1970, 1993, IAA 92-3611, 1992.

(Received 19 Oct. 2010; Accepted 12 Sept. 2011)